

# Optimizing the Imaging Protocol for *Ex Vivo* Coronary Artery Wall Using High-Resolution MRI: An Experimental Study on Porcine and Human

Jiong Yang, MD<sup>1</sup>, Tao Li, MD, PhD<sup>2</sup>, Xiaoming Cui, BS<sup>2</sup>, Weihua Zhou, BS<sup>2</sup>, Xin Li, MD<sup>2</sup>, Xinwu Zhang, MD<sup>3</sup>

Departments of <sup>1</sup>Medical, <sup>2</sup>Radiology and <sup>3</sup>Pathology, The General Hospital of Chinese People's Armed Police Forces, Beijing 100039, China

**Objective:** To optimize the MR imaging protocol for coronary arterial wall depiction *in vitro* and characterize the coronary atherosclerotic plaques.

**Materials and Methods:** MRI examination was prospectively performed in ten porcine hearts in order to optimize the MR imaging protocol. Various surface coils were used for coronary arterial wall imaging with the same parameters. Then, the image parameters were further optimized for high-resolution coronary wall imaging. The signal-noise ratio (SNR) and contrast-noise ratio (CNR) of images were measured. Finally, 8 human cadaver hearts with coronary atherosclerotic plaques were prospectively performed with MRI examination using optimized protocol in order to characterize the coronary atherosclerotic plaques.

**Results:** The SNR and CNR of MR image with temporomandibular coil were the highest of various surface coils. High-resolution and high SNR and CNR for *ex vivo* coronary artery wall depiction can be achieved using temporomandibular coil with 512 x 512 in matrix. Compared with histopathology, the sensitivity and specificity of MRI for identifying advanced plaques were: type IV-V (lipid, necrosis, fibrosis), 94% and 95%; type VI (hemorrhage), 100% and 98%; type VII (calcification), 91% and 100%; and type VIII (fibrosis without lipid core), 100% and 98%, respectively.

**Conclusion:** Temporomandibular coil appears to be dramatically superior to eight-channel head coil and knee coil for *ex vivo* coronary artery wall imaging, providing higher spatial resolution and improved the SNR. *Ex vivo* high-resolution MRI has capability to distinguish human coronary atherosclerotic plaque compositions and accurately classify advanced plaques.

**Index terms:** Coronary vessels; Magnetic resonance imaging; Atherosclerosis; Pathology

## INTRODUCTION

Studies have shown that most acute coronary syndromes (ACS) result from the rupture of unstable plaques and

subsequent thrombus formation (1, 2). The risk of atherosclerotic plaque disruption and thrombosis is thought to be closely related to plaque composition rather than the severity of an actual luminal stenosis (3-5). Therefore, it is of paramount clinical importance to elucidate the composition of coronary atherosclerotic plaques.

The atherosclerotic plaque imaging is the arterial wall imaging (6, 7). Atherosclerosis is a systemic disease of the vessel wall that occurs frequently in the aorta and in the carotid, coronary and peripheral arteries. The formation and development of the atherosclerotic plaque is at the arterial intima. A number of publications (8-10) showed that *vivo* and *ex vivo* MR imaging can characterize the composition of great vessels, such as carotid and aortic atherosclerotic plaques. However, imaging the coronary artery wall with

Received September 15, 2012; accepted after revision March 24, 2013.

**Corresponding author:** Tao Li, MD, PhD, Department of Radiology, The General Hospital of Chinese People's Armed Police Forces, 69 Yongding Road, Beijing 100039, China.

• Tel: (8610) 57976742 • Fax: (8610) 57976742

• E-mail: litaofeivip@163.com

This is an Open Access article distributed under the terms of the Creative Commons Attribution Non-Commercial License (<http://creativecommons.org/licenses/by-nc/3.0>) which permits unrestricted non-commercial use, distribution, and reproduction in any medium, provided the original work is properly cited.

magnetic resonance *in vivo* is challenging due to the cardiac and respiratory motion artifacts, smaller size and tortuous course. Currently, bright blood technique is usually used in imaging human coronary artery *in vivo* (11). Although the black blood technique was used in human coronary artery studies *in vivo* (12-14), only coronary wall thickening could be delineated but the compositions of coronary atherosclerotic plaque were not identified. Poor spatial resolution is another limitation for MRI when identifying coronary atherosclerotic plaque composition *in vivo*. *Ex vivo* coronary artery wall imaging eliminates the above mentioned disadvantages. But the studies were minimal and the procedure was complicated, the coronary artery was dissected from heart (15, 16). Recent study demonstrated that *ex vivo* MRI imaging can classify the human coronary atherosclerotic plaques (17). The general purpose of the present study is to investigate the feasibility and optimize imaging protocol for *ex vivo* porcine and human coronary artery wall using MRI, thus, potentially directing *vivo* MR vessel wall imaging techniques for characterizing coronary atherosclerotic plaques.

## MATERIALS AND METHODS

### Porcine *Ex Vivo* Heart Specimens and Contrast Agent Preparation

Initially, to derive optimal protocol for *ex vivo* coronary artery wall imaging, 10 fresh porcine hearts (weighted from 500 g to 750 g) were prospectively studied with MRI on the day of explanation. The study was approved by the institutional animal care committee. The animals had no suspect of atherosclerotic vessel wall changes. Before examination, the heart was flushed with water to clear clots within the chambers and coronary arteries, and then, a three-way tube was inserted into the left main coronary artery through the left coronary sinus and fixed in order to inject the contrast. To null the lumen and improve the contrast between the wall and lumen, 20 mL of diluted MRI contrast medium containing iron-oxide particles ferucarbotran (Resovist®, SPIO, Bayer Schering Pharma, Berlin, Germany) was injected into the LAD via the three-way tube, mimicking black blood technique. The optimal proportion of MR contrast agent and saline solution was 1% vs. 99% (17).

### Optimizing MR Imaging Procedure

The porcine heart was imaged by using the SIGNA 1.5T

HD MR scanner (GE Medical Systems). To investigate optimal coronary vessel wall delineation, three different surface coils were respectively used as described in Table 1 (temporomandibular surface coil, eight-channel head surface coil and knee coil). The proximal segment of left anterior descending artery (LAD) was placed horizontally. The 3-planar imaging was used for the localization and 3D steady state free precession (SSFP) sequence was used to delineate LAD with repeat time (TR) 7.5 ms, echo time (TE) 3.1 ms, field of view (FOV) 12 x 12 cm, slice thickness 3.0 mm, slice space 1.5 mm, matrix 256 x 192, number of excitations (NEX) 1 (Fig. 1). Before scanning, 10 mL saline solution was injected into the left coronary artery via a three-way tube. Then, 2D spin-echo T1-weighted image (T1WI) with fat saturation was performed respectively with temporomandibular surface coil, eight-channel head surface coil and knee coil using the same parameters (TR 440 ms,

**Table 1. SNR and CNR of T1WI Using Different Coils**

Coil	Matrix	NEX	SNR	CNR1	CNR2
Head coil	384 x 256	3	12.06	4.70	6.49
Knee coil	384 x 256	3	14.42	5.30	9.06
Temporomandibular coil	384 x 256	3	72.89	18.18	53.32
Temporomandibular coil	512 x 512	3	34.18	11.72	24.85
<i>P</i> value			< 0.05	< 0.05	< 0.05

**Note.** — Head coil = eight-channel head coil, SNR = signal noise ratio, CNR = contrast noise ratio, NEX = number of excitations, CNR1 = between LAD wall and lumen, CNR2 = between LAD wall and surrounding fatty tissue

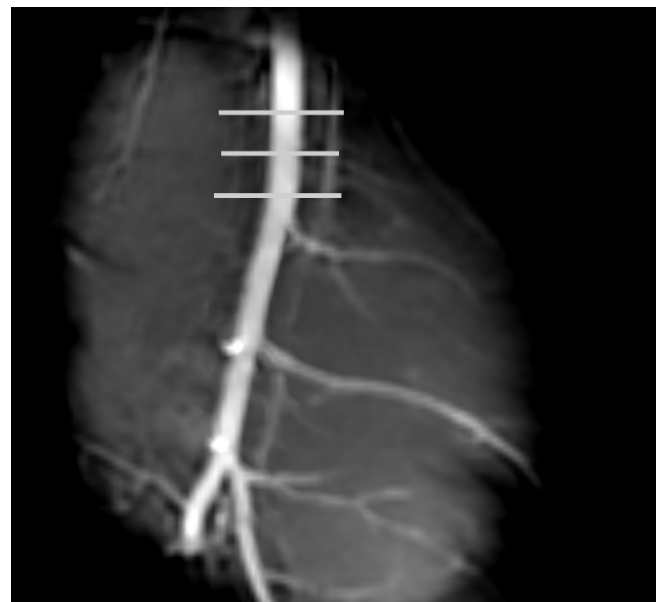


**Fig. 1. Three dimensional steady state free precession sequence imaging left anterior descending artery (LAD) as scout for LAD short axial imaging.**

TE 21 ms, FOV 12 x 9 cm, slice 2 mm, slice space 0.2 mm, matrix 384 x 256, a resolution in-plane of 313 x 352  $\mu$ m, 3 signal averages). Fat suppression was used to reduce the signals from epicardial fatty tissues. The purpose of using different coil imaging 2D spin-echo T1W1 was to select the coil with the highest SNR image.

Next, 2D spin-echo T1WI was repeated with temporomandibular surface coil and matrix 512 x 512 (same other parameters). The purpose of using 512 x 512 in matrix was to investigate if the SNR and CNR of the images were acceptable on the basis of higher spatial resolution. Lastly, T1WI, proton density-weighted image (PDWI) and fast spin echo T2-weighted image (FSE T2WI) with fat saturation, were performed by using temporomandibular surface coil after MR contrast injection. The orientation of T1WI, PDW and T2WI was coincident. The parameters of T1WI were TR 440 ms, TE 21 ms, FOV 12 x 9 cm, slice 2 mm, slice space 0.2 mm, matrix 512 x 512, a resolution in-plane of 234 x 176  $\mu$ m, 3 signal averages. The parameters of PDW included TR 2000 ms, TE 21 ms, FOV 12 x 9 cm, slice 2 mm, slice space 0.2 mm, matrix 512 x 512, 3 signal averages. The parameters of T2WI were TR 4500 ms, TE 105 ms, FOV 12 x 9 cm, slice 2 mm, slice space 0.2 mm, matrix 512 x 512, 3 signal averages.

### Human *Ex Vivo* Heart Specimens

The study was approved by our institutional review board. The informed consents were available from the relatives of the deceased. The hearts from 8 consecutive autopsy subjects with known coronary artery diseases (8 males aged from 84 to 90 years with a mean age of  $86.3 \pm 1.4$  years, 4 died from malignancy, 3 from infections and 1 with myocardial infarction) underwent the coronary MR examinations. The time interval between patient's death and MR imaging was within 24 hours. The specimen preparation was identical to the modality used for porcine hearts. The imaging protocols were described above, with temporomandibular surface coil and matrix 512 x 512. Although the SNR and CNR with 512 x 512 images in matrix were lower than those with 384 x 256 in matrix (the increase in matrix and spatial resolution will consequentially sacrifice SNR) using temporomandibular surface coil, spatial resolution was remarkably increased and image quality was better than the 384 x 256 in matrix with eight-channel head coil and knee coil. Therefore, we imaged human coronary artery wall with temporomandibular surface coil and 512 x 512 in matrix. After scanning,

standard pathological sectioning of human hearts were performed immediately. The proximal 40 mm of the LAD was sectioned into 10 tissue blocks of 4 mm in thickness, and the distance from the tissue block to the bifurcation of the left main coronary artery was recorded to match with MR images. After decalcification, the tissue blocks were embedded in paraffin and prepared for histological examination in sections 4- $\mu$ m thick. Blocks were stained with haematoxyline and eosin (HE).

### Analysis of MR Data

#### *Porcine Hearts*

To test the optimal protocol for *ex vivo* coronary artery wall imaging, the proximal segment of LAD in porcine heart was chosen as a target vessel. Signals of the LAD wall, lumen, surrounded by fatty tissues adjacent to LAD, myocardium of anterior part of interventricular septum and noise were respectively measured. Noise was the standard deviation of air signal intensity. SNR of image, CNR1 between the LAD wall and lumen, CNR2 between the LAD wall and surrounding fatty tissue were respectively calculated. The equations were as follow.

$$\text{SNR} = \frac{\text{The signal of myocardium of anterior part of interventricular septum}}{\text{Noise (the standard deviation of air signal intensity)}}$$

$$\text{CNR1} = \frac{\text{The signal of LAD wall minus the signal of lumen}}{\text{Noise (the standard deviation of air signal intensity)}}$$

$$\text{CNR2} = \frac{\text{The signal of LAD wall minus the signal of surrounding fatty tissue}}{\text{Noise (The standard deviation of air signal intensity)}}$$

#### *Human Ex Vivo Hearts*

To test the delineation of atherosclerotic plaque, the *ex vivo* human hearts were evaluated. Two experienced radiologist, blinded to the histopathology results, evaluated the original two-dimensional, cross-sectional MR images independently and collectively resolved any differences in reading. Each reader classified the plaque independently twice, 2 months apart, to determine the intra-observer variability. The thickness of the vessel wall and signal of plaque were recorded. The plaques were classified according to the AHA criteria and modified the histological classification by Cai et al. (18-20). MRI cannot distinguish type IV lesion from type V lesion, so they are called type IV-V (lipid, necrosis, fibrosis) lesion. Type IV-V lesions

showed high or equal signal intensity on T1WI and PDW, low or equal signal intensity on T2WI. Type VI (sub-acute hemorrhage) lesions showed high signal intensity on T1WI and T2WI. Type VII (calcification) lesions showed signal loss on all three sequences. Type VIII (fibrosis without lipid core) lesions had equal signal intensity on T1WI and high or equal signal intensity on T2WI. For each image location, there were three images (T1WI, PDW, T2WI) available for reviews to determine the lesion type. To decrease dependence on lesion type, MR images of proximal 40 mm of LAD were selected at a 4-mm interval (originally 14-20 images, selected 1 from 2 images). This protocol generated 7 to 10 image locations per LAD that could be compared with histological sections. The histopathologic sections were analyzed by an experienced pathologist who was blinded to the MRI results, and plaques were classified according to the AHA criteria (19, 20). I.e., type IV-V (lipid, necrosis, fibrosis); type VI (hemorrhage); type VII (calcification) and type VIII (fibrosis without lipid core). MRI images and histopathologic sections were matched prospectively in the region of the proximal 40 mm of the LAD. The process of matching images to histopathologic sections used landmarks such as the relative distance from the left main trunk bifurcation, and some morphological features such as vessel shapes and lumen sizes, the location of the LAD branches, as well as calcifications.

### Statistical Analysis

For the porcine hearts, comparisons of the SNR, CNR1, CNR2 of T1WI using temporomandibular surface coil, eight-channel head surface coil and knee coil were performed using analysis of variance, with  $p$ -value  $< 0.05$  considered statistically significant. Comparisons of the SNR and CNR of T1WI using temporomandibular surface coil with different

matrix were performed using analysis of variance.

For the human hearts, the sensitivity, specificity and accuracy of MRI for classifying the plaques were calculated. To test for intra-observer and inter-observer agreements of MRI-based plaque classification, the kappa statistics ( $k$ ) were used.

## RESULTS

### Porcine Coronary Artery

The SNR, CNR1 and CNR2 of T1WI using temporomandibular surface coil, eight-channel head surface coil and knee coil were summarized in Table 1. The SNR, CNR1 and CNR2 of T1WI using temporomandibular surface coil were higher than those using eight-channel head surface coil and knee coil ( $p < 0.05$ ) (Fig. 2). The SNR and CNR2 of T1WI using knee coil were higher than those using eight-channel head surface coil ( $p < 0.05$ ). However, the CNR1 of T1WI using knee coil was higher than that using eight-channel head surface coil and did not reach statistical significance ( $p > 0.05$ ). The SNR and CNR1 and CNR2 of T1WI with 512 x 512 in matrix using temporomandibular surface coil were lower than those with 384 x 256 in matrix ( $p < 0.05$ ) (Fig. 3), but markedly higher than those using eight-channel head coil and knee coil with 384 x 256 in matrix ( $p < 0.05$ ). Accordingly, the image quality of T1WI, PDW and T2WI with 512 x 512 in matrix using temporomandibular surface coil was still satisfactory due to the coronary artery wall visualized clearly, accompanying higher spatial resolution compared with 384 x 256 in matrix (Fig. 4).

### Human Coronary Artery

A total of 58 MRI images from the 8 hearts were matched

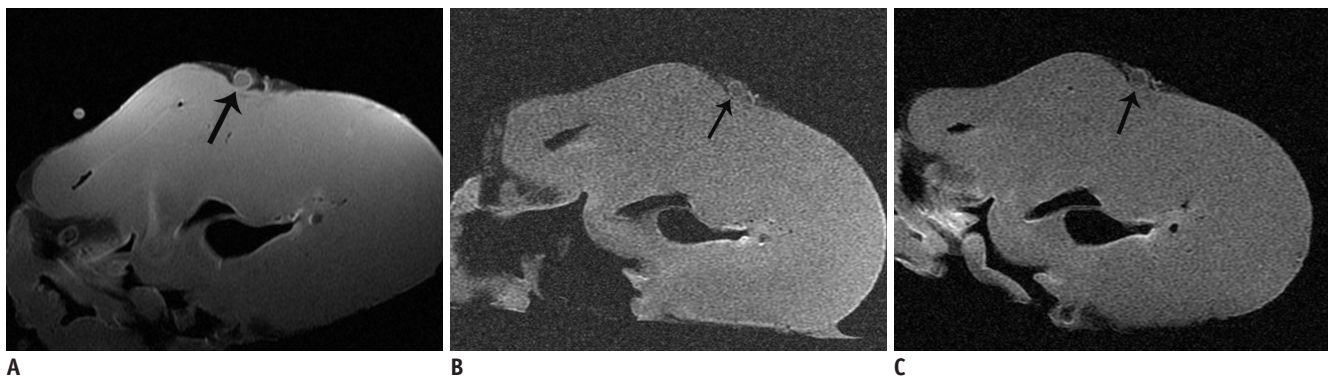
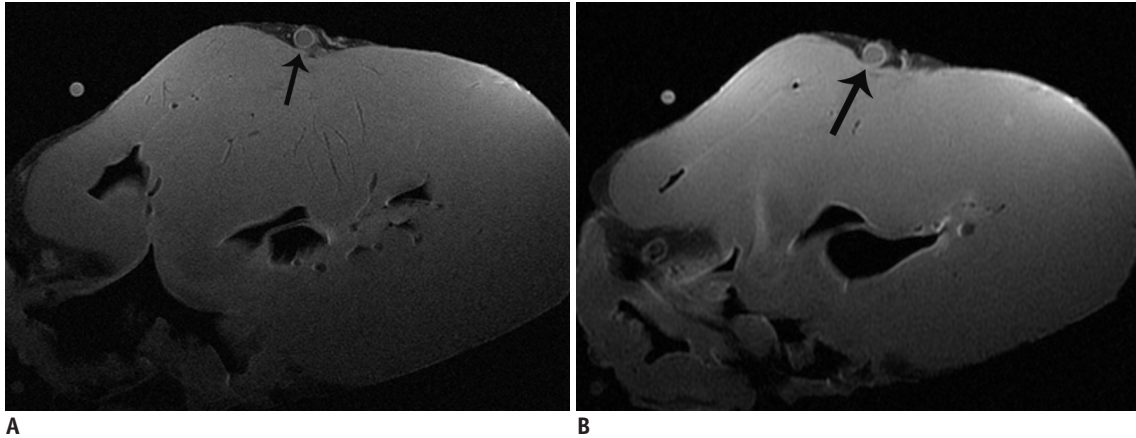


Fig. 2. Signal noise ratio, and CNR between left anterior descending artery wall and lumen, of T1 weighted image, using temporomandibular surface coil (A) were higher than those of head coil (B) and knee coil (C) with same parameters, 384 x 256 in matrix.

with corresponding histopathologic sections. Among the histopathologic sections, there were 18 lipid-rich plaque sections (type IV-V) (31%) (Fig. 5), 4 hemorrhage plaque

sections (type VI) (7%) (Fig. 6), 33 calcified plaque sections (type VII) (57%) (Fig. 7), and 3 fibrous plaque sections (type VIII) (5%) (Fig. 8).



**Fig. 3.** Signal noise ratio, and CNR between left anterior descending artery wall and lumen, of T1 weighted image, with 512 x 512 in matrix (A) using temporomandibular surface coil were lower than those with 384 x 256 in matrix (B), however coronary artery wall was demonstrated more clearly.

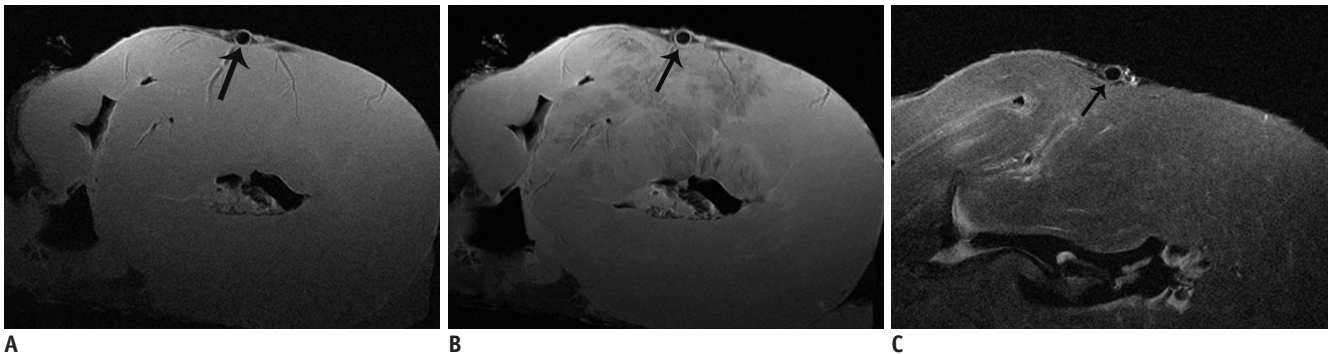


**Fig. 4.** Image quality of T1 weighted image (A), proton density-weighted image (B) and T2-weighted image (C) with 512 x 512 in matrix was still satisfactory using temporomandibular surface coil, accompanying higher spatial resolution compared with 384 x 256 in matrix. Coronary artery wall was visualized clearly (black arrow) and noise was acceptable.

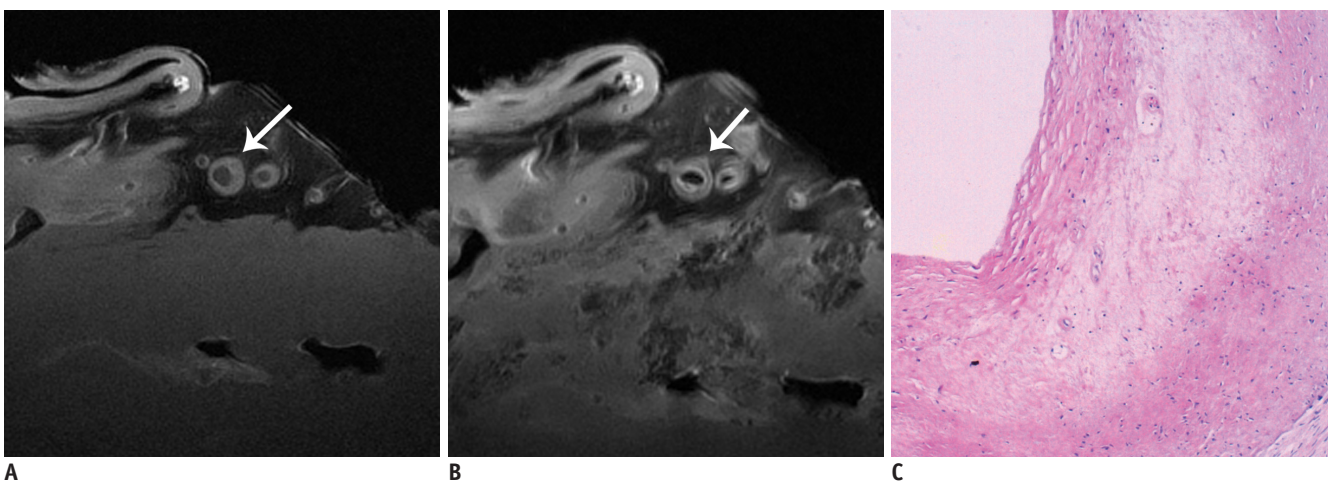


**Fig. 5. Type IV-V lesion.**

MRI images (A, B) showed irregular thickening of left anterior descending artery wall, slightly high or equal signal on T1 weighted image (A), and slightly low signal on proton density-weighted (B) (white arrow in A and B). Pathological section showed extracellular lipid accumulating into lipid pool (C). Original magnification was x 4.

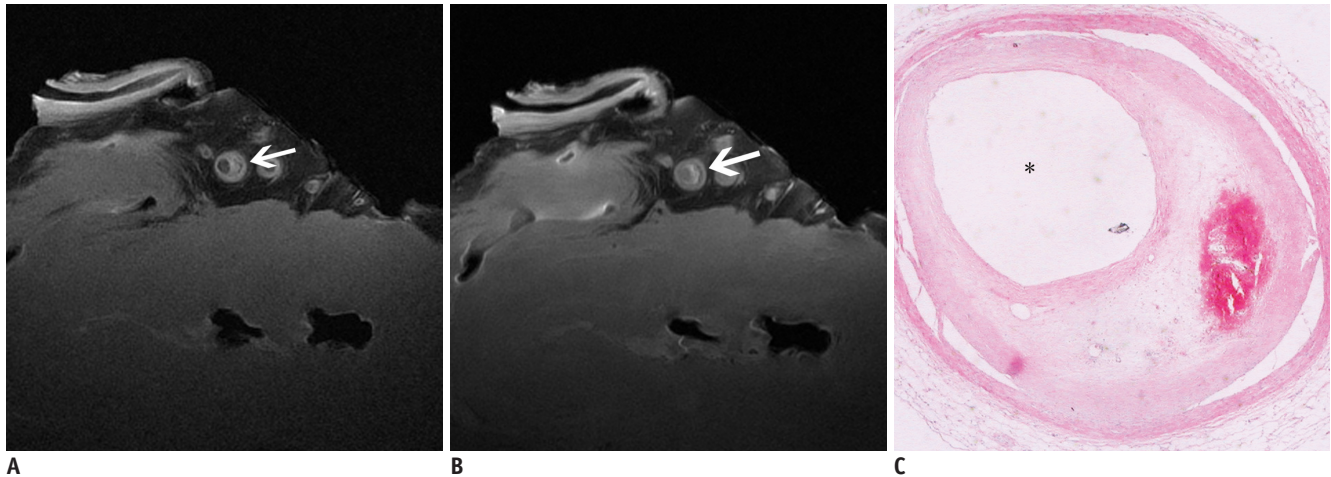


**Fig. 6. Type VI lesion with intraplaque hemorrhage.**

Plaque showed high signal on T1 weighted image (A) and proton density-weighted (B) (white arrow in A and B). Pathological section showed intraplaque hemorrhage (C). Original magnification was x 4.

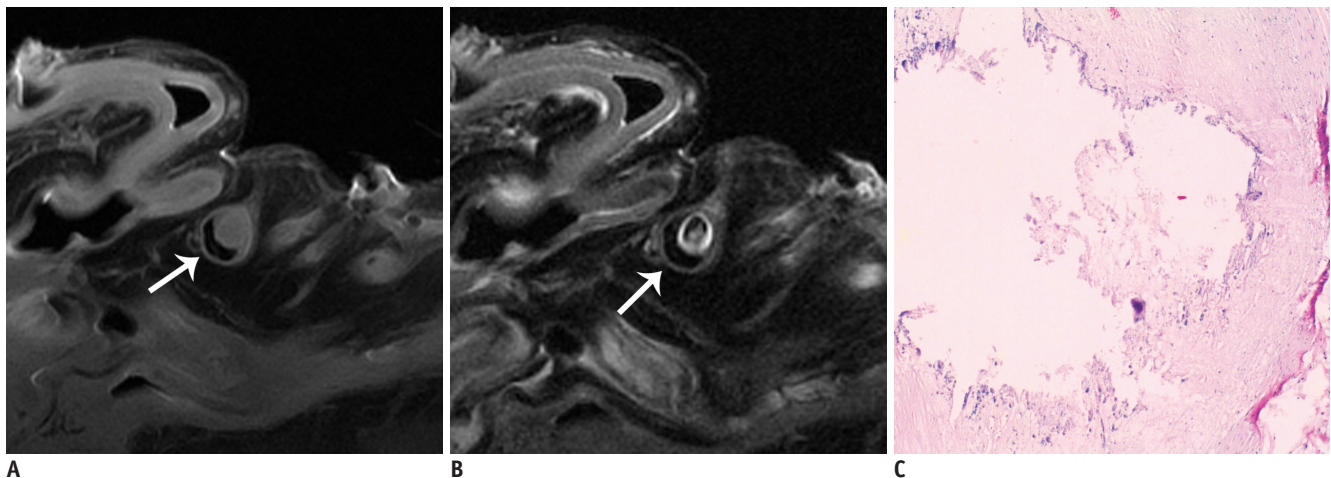


**Fig. 7. Type VII lesion, densely calcified plaque.**

Calcified plaque presented low signal on proton density-weighted (A) and T2-weighted image (B) (white arrow in A and B). Calcification was evident in pathological section (C). Original magnification was x 4.

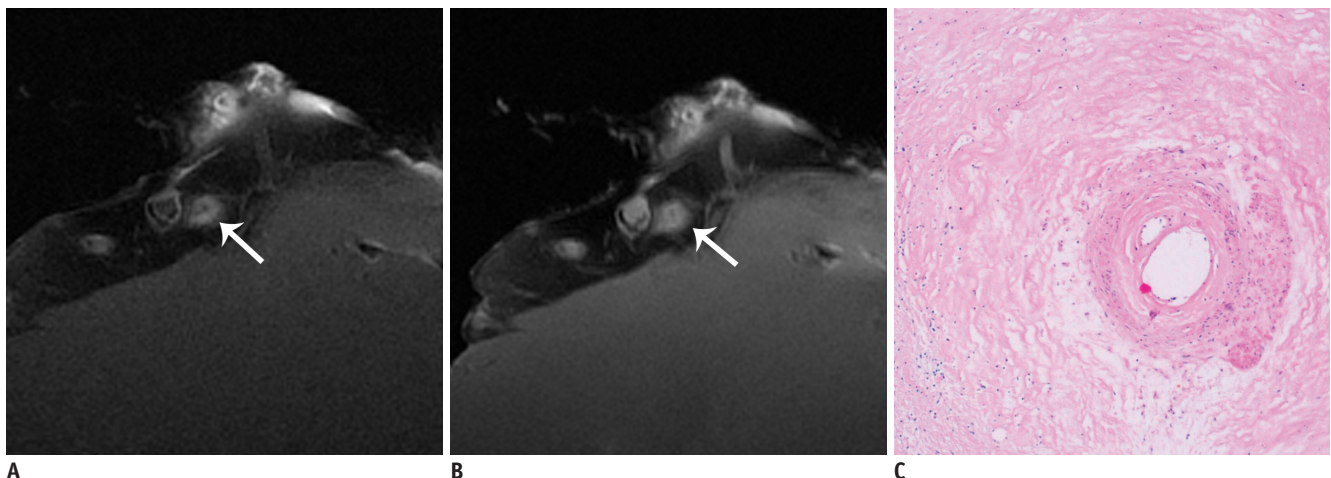


**Fig. 8. Type VIII lesion, fibrous plaque.**

Fibrous plaque presented equal signal intensity on T1 weighted image (A) and high signal intensity on T2WI (B) (white arrow in A and B). Fibrous tissue was evident in pathological section (C). Original magnification was x 4.

**Table 2. MRI and Histopathologic Classifications of Coronary Atherosclerotic Plaques**

MR \ Pathology	IV-V	VI	VII	VIII	Total
IV-V	17	-	2	-	19
VI	-	4	1	-	5
VII	-	-	30	-	30
VIII	1	-	-	3	4
Total	18	4	33	3	58

**Note.** — type IV-V (lipid, necrosis, fibrosis), type VI (hemorrhage), type VII (calcification), type VIII (fibrosis without lipid core)

The accuracy of MRI for classification of plaques was 93% (54/58), and the distribution of plaques was shown in Table 2. The sensitivity and specificity of MRI for identifying different types of plaques were: type IV-V, 94% and 95%; type VI, 100% and 98%; type VII, 91% and 100%; and type VIII, 100% and 98%, respectively. Intra-observer agreement among two readers for two readings with 2 months apart was excellent ( $k = 0.85$  and  $k = 0.83$ ). Agreement between two readers was also very good for plaque classification ( $k = 0.8$ ).

## DISCUSSION

The major findings of the study were 2-folded: firstly, we found that visualizing the coronary artery wall *in vitro* using temporomandibular surface coil was of the highest SNR and CNR; secondly, we demonstrated that high-resolution MRI closely agrees with histopathology in the detection of human coronary atherosclerotic plaques compositions and classification of plaques.

The 2.5-inch temporomandibular surface coil is dramatically superior to eight-channel head surface coil and knee coil in *ex vivo* coronary artery wall imaging. However, knee coil was commonly used in *ex vivo* coronary artery imaging with magnetic resonance techniques in previous literatures (6, 21). The SNR and CNR of small objects such as coronary arterial wall are improved as the diameter of surface coil decreases. The 2.5-inch temporomandibular surface coil is dramatically smaller than eight-channel head surface coil and knee coil, and matches very well with the coronary artery. Therefore, we used the temporomandibular surface coil and the SNR and CNR of coronary artery wall imaging were markedly higher than those using eight-channel head surface coil and knee coil. To our knowledge, this is the first report to image coronary artery wall *ex vivo* using temporomandibular surface coil.

*Ex vivo* high-resolution MRI was able to distinguish human

coronary atherosclerotic plaque composition and accurately classify advanced plaques. Based on composition, the AHA classifies coronary atherosclerotic plaques into 8 different types (19, 20). Type I-III plaques belong to early lesions, which can be dissipated; and type IV-VIII plaques belong to advanced lesions. Type IV-V (lipid, necrosis, fibrosis) lesions showed high or equal signal intensity on T1WI and PDW, low or equal signal intensity on T2WI. Type VI (sub-acute hemorrhage) lesions showed high signal intensity on T1WI and T2WI. Type VII (calcification) lesions showed signal loss on all three sequences. Type VIII (fibrosis without lipid core) lesions had equal signal intensity on T1WI and high or equal signal intensity on T2WI. In this study, the sensitivity and specificity of MRI for classifying advanced plaques were high (type IV-V, 94% and 95%; type VI, 100% and 98%; type VII, 91% and 100%; and type VIII, 100% and 98%, respectively).

There are a few limitations in this study. Firstly, *ex vivo* high-resolution MR imaging techniques can be further optimized. One method is using the high-field MRI scanner, in which SNR and spatial resolution can be further improved (22, 23). Secondly, the number of fibrous plaques was limited because type VIII lesions are rare and may have a potential influence on the assessment of type VIII lesions. Thirdly, the whole coronary arteries including RCA and LCX can't be covered because the temporomandibular surface coil is smaller than the knee joint and head coils.

## Conclusions

Temporomandibular surface coil was dramatically superior to eight-channel head coil and knee coil for *ex vivo* coronary artery wall imaging, providing for higher spatial resolution and improved SNR with 512 x 512 in matrix. *Ex vivo* high-resolution MRI was able to distinguish human coronary atherosclerotic plaque compositions and accurately classify advanced plaques, which may be helpful for directing the development and optimizing the *vivo* MR vessel wall imaging techniques for characterizing coronary atherosclerotic plaques.

## REFERENCES

1. Falk E, Shah PK, Fuster V. Coronary plaque disruption. *Circulation* 1995;92:657-671
2. Virmani R, Burke AP, Farb A, Kolodgie FD. Pathology of the vulnerable plaque. *J Am Coll Cardiol* 2006;47(8 Suppl):C13-C18
3. Fuster V, Badimon L, Badimon JJ, Chesebro JH. The pathogenesis of coronary artery disease and the acute

- coronary syndromes (1). *N Engl J Med* 1992;326:242-250
4. Fuster V, Badimon L, Badimon JJ, Chesebro JH. The pathogenesis of coronary artery disease and the acute coronary syndromes (2). *N Engl J Med* 1992;326:310-318
  5. Virmani R, Kolodgie FD, Burke AP, Farb A, Schwartz SM. Lessons from sudden coronary death: a comprehensive morphological classification scheme for atherosclerotic lesions. *Arterioscler Thromb Vasc Biol* 2000;20:1262-1275
  6. Nikolaou K, Becker CR, Flohr T, Huber A, Scheidler J, Fayad ZA, et al. Optimization of ex vivo CT- and MR- imaging of atherosclerotic vessel wall changes. *Int J Cardiovasc Imaging* 2004;20:327-334
  7. Stary HC, Blankenhorn DH, Chandler AB, Glagov S, Insull W Jr, Richardson M, et al. A definition of the intima of human arteries and of its atherosclerosis-prone regions. A report from the Committee on Vascular Lesions of the Council on Arteriosclerosis, American Heart Association. *Circulation* 1992;85:391-405
  8. Yuan C, Mitsumori LM, Ferguson MS, Polissar NL, Echelard D, Ortiz G, et al. In vivo accuracy of multispectral magnetic resonance imaging for identifying lipid-rich necrotic cores and intraplaque hemorrhage in advanced human carotid plaques. *Circulation* 2001;104:2051-2056
  9. Yuan C, Kerwin WS, Ferguson MS, Polissar N, Zhang S, Cai J, et al. Contrast-enhanced high resolution MRI for atherosclerotic carotid artery tissue characterization. *J Magn Reson Imaging* 2002;15:62-67
  10. Fayad ZA, Nahar T, Fallon JT, Goldman M, Aguinaldo JG, Badimon JJ, et al. In vivo magnetic resonance evaluation of atherosclerotic plaques in the human thoracic aorta: a comparison with transesophageal echocardiography. *Circulation* 2000;101:2503-2509
  11. Gweon HM, Kim SJ, Lee SM, Hong YJ, Kim TH. 3D whole-heart coronary MR angiography at 1.5T in healthy volunteers: comparison between unenhanced SSFP and Gd-enhanced FLASH sequences. *Korean J Radiol* 2011;12:679-685
  12. Kim WY, Astrup AS, Stuber M, Tarnow L, Falk E, Botnar RM, et al. Subclinical coronary and aortic atherosclerosis detected by magnetic resonance imaging in type 1 diabetes with and without diabetic nephropathy. *Circulation* 2007;115:228-235
  13. Macedo R, Chen S, Lai S, Shea S, Malayeri AA, Szklo M, et al. MRI detects increased coronary wall thickness in asymptomatic individuals: the multi-ethnic study of atherosclerosis (MESA). *J Magn Reson Imaging* 2008;28:1108-1115
  14. Gerretsen S, Kessels AG, Nelemans PJ, Dijkstra J, Reiber JH, van der Geest RJ, et al. Detection of coronary plaques using MR coronary vessel wall imaging: validation of findings with intravascular ultrasound. *Eur Radiol* 2013;23:115-124
  15. Serfaty JM, Chaabane L, Tabib A, Chevallier JM, Briguet A, Douek PC. Atherosclerotic plaques: classification and characterization with T2-weighted high-spatial-resolution MR imaging-- an in vitro study. *Radiology* 2001;219:403-410
  16. Yuan C, Hatsukami TS, O'Brien KD. High-Resolution magnetic resonance imaging of normal and atherosclerotic human coronary arteries ex vivo: discrimination of plaque tissue components. *J Investig Med* 2001;49:491-499
  17. Li T, Li X, Zhao X, Zhou W, Cai Z, Yang L, et al. Classification of human coronary atherosclerotic plaques using ex vivo high-resolution multicontrast-weighted MRI compared with histopathology. *AJR Am J Roentgenol* 2012;198:1069-1075
  18. Cai JM, Hatsukami TS, Ferguson MS, Small R, Polissar NL, Yuan C. Classification of human carotid atherosclerotic lesions with in vivo multicontrast magnetic resonance imaging. *Circulation* 2002;106:1368-1373
  19. Stary HC, Chandler AB, Glagov S, Guyton JR, Insull W Jr, Rosenfeld ME, et al. A definition of initial, fatty streak, and intermediate lesions of atherosclerosis. A report from the Committee on Vascular Lesions of the Council on Arteriosclerosis, American Heart Association. *Circulation* 1994;89:2462-2478
  20. Stary HC, Chandler AB, Dinsmore RE, Fuster V, Glagov S, Insull W Jr, et al. A definition of advanced types of atherosclerotic lesions and a histological classification of atherosclerosis. A report from the Committee on Vascular Lesions of the Council on Arteriosclerosis, American Heart Association. *Circulation* 1995;92:1355-1374
  21. Nikolaou K, Becker CR, Muders M, Babaryka G, Scheidler J, Flohr T, et al. Multidetector-row computed tomography and magnetic resonance imaging of atherosclerotic lesions in human ex vivo coronary arteries. *Atherosclerosis* 2004;174:243-252
  22. Koops A, Ittrich H, Petri S, Priest A, Stork A, Lockemann U, et al. Multicontrast-weighted magnetic resonance imaging of atherosclerotic plaques at 3.0 and 1.5 Tesla: ex-vivo comparison with histopathologic correlation. *Eur Radiol* 2007;17:279-286
  23. Cury RC, Houser SL, Furie KL, Stone JR, Ogilvy CS, Sherwood JB, et al. Vulnerable plaque detection by 3.0 tesla magnetic resonance imaging. *Invest Radiol* 2006;41:112-115